CHAPTER

9

Fugacity Models

X.-Z. Kong, F.-L. Xu[1], W. He, W.-X. Liu, B. Yang

Peking University, Beijing, China

[1]Corresponding author: E-mail: xufl@urban.pku.edu.cn

OUTLINE

http://dx.doi.org/10.1016/B978-0-444-63623-2.00009-8

9.1 FUGACITY MODELS: DEVELOPMENT AND APPLICATIONS

9.1.1 Introduction of Fugacity Models

Multimedia models were mathematical models for description of chemical behavior that was being rapidly developed since the 1980s (Cohen, 1984). These models were built based on the principles that the fate, transport, and transformation of the chemicals were determined by both environmental factors and physical–chemical properties. The most important processes for transport and transformation within and between compartments are incorporated. As a result, multimedia models for chemicals were applied abundantly in both ecological and environmental researches, such as biogeochemical studies of pollutants, ecological risk assessment, and environmental management. Multiple types of multimedia models were proposed. Representatives of these models are TOXIC model (Schnoor and Mcavoy, 1981), EXAMS model (Burns et al., 1982; Yoshida et al., 1987), and PRZM model (Carsel et al., 1984). Among all these multimedia models, fugacity models are one of the most successful types due to its simplicity in structure and accessible in parameterization (Mackay, 2001).

9.1.2 Development and Applications of Fugacity Models

Fugacity evaluates the equilibrium distribution and tendency of chemicals to escape between phases (Mackay and Paterson, 1981). Fugacity was firstly introduced into chemical modeling in the beginning of the 1980s (Mackay, 1979; Mackay and Paterson, 1981, 1982b). There are four levels in fugacity model in total (Levels I–IV) with increasing complexity (Mackay and Paterson, 1982b). Level I model is for equilibrium, stable, and nonflowing system; Level II is equilibrium, stable, and flowing system; Level III is nonequilibrium, stable, and flowing system; and Level IV is nonequilibrium, nonstable, and flowing system.

Much works have been done during the development of fugacity models, particularly by the group of Donald Mackay. A Level III model for aquatic ecosystem, including lakes and rivers, was developed and applied to predict the fate and residual levels of organic pollutants in air, water, and sediment (Mackay et al., 1983a,b). The model was subsequently utilized for both organic and inorganic compounds in lakes (Mackay and Diamond, 1989). Moreover, an explicitly model description of air–water interactions was developed (Mackay et al., 1986). As the processes in fugacity model became more precise, the model was validated by more case studies. For example, fate of six chemicals in four environmental compartments (air, water, soil, and sediment) was modeled simultaneously by a Level III fugacity model (Mackay and Paterson, 1991), and the model was subsequently applied in a much larger regional scale (Mackay et al., 1992).

In addition, fugacity models were widely used and continuously modified by researchers around the world, which also played an important role in the model development. Earlier works focused on incorporating major components into fugacity models, most of which were Level III steady state models. These components include biota in food chain and food web in aquatic ecosystem (Connolly and Pedersen, 1988). The bioconcentration, bioaccumulation, and biomagnification effects of organic pollutants were nicely modeled. Moreover, efforts were taken in extending the scales of fugacity models, such as application

to a large group of chemicals (45 priority contaminants from USEPA) with different physical–chemical properties (Edwards et al., 1999), which led to a clearer linkage between chemical properties and their environmental behavior. Deep insights were obtained by considering the effects of spatial heterogeneity in Level III fugacity model ranged from regional (Tao et al., 2003) to global (Ballschmiter, 1992; Wania and Mackay, 1995) scales. It was suggested that the incorporation of spatial variations would decrease the model uncertainty (Tao et al., 2003). In general, applications of Level III models were abundant, focusing on either terrestrial (Parajulee and Wania, 2014; Wang et al., 2002; Wania et al., 2006) or aquatic (Baek and Park, 2000; Wang et al., 2012; Xu et al., 2013) study sites.

Following studies attempted to use Level IV model, the algorithm of which was primarily investigated as the basis for further research (Paraiba et al., 2002, 1999). Level IV fugacity models were applied in both short-term simulation with seasonal variations and long-term simulation with changes in emission intensity. For the short-term, seasonal variations of contaminants were successfully predicted by Level IV fugacity models with a relative low model uncertainty, particularly for polycyclic aromatic hydrocarbon (PAHs) in terrestrial systems (Lang et al., 2007; Wang et al., 2011) and hexachlorocyclohexanes (HCHs) in aquatic systems (Kong et al., 2014, 2012). For the long-term, impact of the changes in organochlorine pesticides (OCPs) application intensity on their environmental residual levels since the 1960s in China have been revealed by fugacity models in regional scales (Ao et al., 2009; Cao et al., 2007; Dong et al., 2009; Kong et al., 2014; Liu et al., 2007; Tao et al., 2006). These applications of fugacity models, which showed a significant model response to the changes in emission rate and a relative good fit of model predictions to measured data, fall within the objectives of Level IV fugacity model (Mackay and Paterson, 1982a). Serving as critical implications, fugacity models are able to predict the residual levels of certain chemicals in the coming decades, such that the concentrations of γ-HCH was predicted to decrease by 1.7–1.9 orders of magnitude in 2020 in Tianjin, China (Tao et al., 2006). Furthermore, it is interesting that spatial and temporal variations are addressed simultaneously in one fugacity model study (Wang et al., 2011). Factors influencing distributions of POPs in a global scale was also illustrated by fugacity models (Wania and Mackay, 1995). This study showed that the temperature was a significant factor, whereas parameters strongly affected by temperature were still poorly modeled. It is also interesting to note that fugacity models were integrated with atmospheric transportation model to account for global distribution and health risk from inhalation exposure of PAHs (Zhang et al., 2009).

Recent studies for fugacity models took great efforts on incorporating submodels for biota phases from different trophic levels, which would lead to a more simple structure of food web accumulation model. These studies were of great importance, because higher chemical concentrations in higher trophic levels may lead to catastrophic consequences (Sharpe and Mackay, 2000), such as the extinction of bird species due to polychlorinated biphenyls (PCBs) biomagnification (Gilbertson, 1996) and increasing health risks of human beings due to dioxin exposure from fish consumption (Thomas et al., 1998). The development of fugacity-based food web accumulation model was, on one hand, based on the quantitative evaluation of bioaccumulation model from earlier researches, which had demonstrated the potential bioaccumulation and biomagnification effects of certain chemicals. For example, relationship between bioaccumulation factor (K_B) and octanol/water partition coefficients (K_{ow}) was built ($K_B = 0.048K_{ow}$), which served as an essential basis for further model

development (Mackay, 1982). On the other hand, it was unraveled that the fugacity ratio between biota and water could be higher than 1, indicating that the fugacity gradient along the trophic level is the key factor for potential bioaccumulation and biomagnification effects (Connolly and Pedersen, 1988). These findings are the theoretical foundation for food web fugacity model.

Fugacity model for food web started from fish (Mackay and Hughes, 1984), and a more detailed model for digestive system in fish was developed, by which digestion and food adsorption in gastrointestinal were both identified as the major mechanisms for biomagnification in food chain (Gobas et al., 1999; Gobas et al., 1993). Uncertainty was also addressed for fish fugacity model to increase accuracy of model prediction (Hauck et al., 2011). As a further step, fugacity models were extended to the whole food chain and food web, resulting in a more systematic description on transport and transformation of chemicals in food webs. The ultimate goal of the model is to predict chemical concentrations in biota from data in abiotic phases and to facilitate the ecological risk assessment of these chemicals. These approaches focused particularly on aquatic ecosystems, e.g., a food chain with six trophic levels, including zoobenthos, plankton, and fish (Diamond et al., 1996). A general framework for fugacity-based food web accumulation model was also developed, which could incorporate N groups in the model with a matrix of N dimensions (Campfens and Mackay, 1997). A case study on PCBs in the Great Lakes showed a good fit of model predictions to field data (deviations within three folds). The fugacity-based food web accumulation model was under continuous modifications and applications, with updated mechanisms embedded (Arnot and Gobas, 2004; Binelli and Provini, 2003; Gobas and Arnot, 2010). In addition, excretion of birds was found to play an important role in driving the fate of chemicals in aquatic ecosystems. Therefore, birds were included in the fugacity models and the framework of evaluation for chemicals in aquatic environment (Sharpe and Mackay, 2000). An interesting study in two high-latitude lakes in Norway showed that rather than food web structure and lake morphology, intensive bird's dropping in one lake was the major reason for the 10-fold higher PCBs concentrations in fish than those in the other lake. Overall, as a synthesis, a three-layer model framework was proposed for a rapid risk assessment of commercial chemicals, which considered the most important components and processes from earlier works via an analytic hierarchy process (Mackay and Fraser, 2000).

Terrestrial and aquatic vegetation were both involved into fugacity models much later than the other components, yet their important roles in driving the fate of chemicals were gradually realized. Vegetation is difficult to model because it has different parts with different functions. For terrestrial vegetation, fugacity-based models were development, as the vegetation was either considered as a whole (Calamari et al., 1987) or divided into leaf, stem, and root (Paterson et al., 1994). Among these modeling approaches, the one for agricultural herbaceous plant was crucial for health risk assessment as they are directly consumed by human beings (Hung and Mackay, 1997). An integrated study reviewed the model and experimental methods for estimating bioconcentration factors (BCFs) for vegetation and showed that uncertainties from the model were relatively larger (McKone and Maddalena, 2007). However, to date, studies focusing on aquatic vegetation are scarce, which remains as a challenge for both experiment and modeling researches (Diepens et al., 2014).

9.1.3 Future Perspectives

The previous section provides a brief review of the development and application of fugacity models. In summary, since the first report of the fugacity models, much effort has been made into the follow three aspects: (1) extending the temporary scale of the model from Levels I to III steady state model to Level IV dynamics model, including both short-term seasonal variations and long-term annual changes; (2) extending the spatial scale of the model from 0-dimension model to those with regional and global variations; (3) incorporating important compartments into the model. In addition to abiotic components such as air, soil, water, and sediment, biota in the system in different trophic levels (from primary producers such as vegetation to top predators such as birds) are incorporated into fugacity models. It has been a great success to combine the knowledge of food chain and food web theory with fugacity models to account for the effects of bioaccumulation and biomagnification of chemicals in the environmental system (Koelmans et al., 2001).

Nonetheless, to date, limitations still exist in the studies for fugacity models. Particularly, these studies were usually regional and were made for the chemical industry to assess whether new chemicals would cause environmental issues or not (Cowan, 1995), whereas models developed for a well-defined ecosystem, e.g., a lake, were rarely reported. However, these types of research are of great importance in that a model evaluation of chemicals behavior in a small scale would provide implications for local managers in environmental risk assessment. In addition, fugacity models were criticized for its poor prediction accuracy and large model uncertainty. Fate of chemicals is determined by many factors so that even one-order magnitude of deviations between model predictions and field data are still acceptable, while uncertainty is still difficult to determine (Cao et al., 2004).

Overall, future studies on fugacity models are suggested in the following three directions: (1) to develop models for a smaller scale. This would require concrete case studies for specific ecosystems (such as lakes), so that the model would be validated by field data and provide a detailed description of the chemical behavior in such systems; (2) to improve model prediction accuracy; ecological and human health risk assessment would benefit more from fugacity models with higher prediction accuracy; (3) to reduce model uncertainty. This would require efforts from two ways. One is incorporating more components into the fugacity models, such as vegetation (Diepens et al., 2014) and dissolved organic matter (Li et al., 2015), so that uncertainty from model structure would be reduced; the other is utilizing advanced statistical methods such as Bayesian-based Markov Chain Monte Carlo (Kong et al., 2014; Saloranta et al., 2008), so that the uncertainty from model parameters would not be overestimated.

9.2 FUGACITY MODEL FOR PAHs IN LAKE SMALL BAIYANGDIAN, NORTHERN CHINA: A CASE STUDY

In the following section, we provide a case study of Level III fugacity model for description of environmental behavior of 15 priority PAHs in a vegetation-dominant lake in China. Aquatic plants were included in the model. The reliability of the model estimates was evaluated by various means, including concentration validation, sensitivity, and uncertainty

analysis. Therefore, this case study provides a nice example of fugacity model for a well-defined ecosystem within a significantly small scale, with many efforts in increasing model performance.

9.2.1 Polycyclic Aromatic Hydrocarbons

PAHs are globally concerned pollutants due to their widespread occurrence, strong persistence, long-range transportation potential, and carcinogenic toxicity (Xu et al., 2011). As one of the fastest growing countries in the world, China is suffering from severe contamination of PAHs from various sources (Zhang et al., 2007). The threat of PAH pollution to ecosystems and human health have become serious in China. It was reported that the atmospheric emissions of 16 priority PAHs in China in 2004 (114 Gg) accounted for about 22% of the total global emissions (520 Gg) of 16 priority PAHs set by USEPA (Zhang et al., 2009). It was estimated that 5.8% of China's land area, where 30% of the population lives, exceeded the national ambient benzo[a]pyrene (BaP) standard of 10 ng/m^3 and that the overall population attributable fraction for lung cancer caused by inhalation exposure to PAHs was 1.6% (Zhang et al., 2009). Therefore, it is meaningful to understand and predict the fate and transport of PAHs in various environmental media in China.

To date, two fugacity model studies included all 16 principal PAHs (Lang et al., 2007; Wang et al., 2011), while specific PAH components such as BaP and phenanthrene (Phe) were considered in other studies (Tao et al., 2003; Wang et al., 2002). However, the fate of PAH components in water and sediments were not well modeled in such studies at regional scales. To solve this limitation, a quantitative water–air sediment interaction (QWASI) fugacity model is strongly required (Mackay et al., 1983a,b). The QWASI fugacity model has been successively applied to predict the fate of heavy metals and organic chemicals such as PCBs and BaP in lake or river ecosystems (Diamond et al., 1996; Mackay et al., 1983a,b). However, priority PAH components other than BaP have not been included in the QWASI fugacity models. To understand properly and to compare the behaviors of individual PAH components in aquatic ecosystems, it is critical to include other priority PAH components excluding BaP, because the behaviors and physical–chemical features are varied for different PAH components (Zhang et al., 2005). Even for BaP, more case studies on using QWASI fugacity model are still needed to understand and predict its fate behaviors in lake ecosystems, especially in such a lake as Small Baiyangdian that has abundant aquatic plants. In the previous studies on the development and application of QWASI fugacity model, aquatic plants were not included.

9.2.2 Study Area and Measurements

Lake Baiyangdian, the largest freshwater lake in Northern China, is located at the central place of three big cities, Beijing, Tianjing, and Shijiazhuang (Fig. 9.1), one of the most seriously polluted areas in China for PAHs (Zhang et al., 2007). Lake Baiyangdian is one of the important locations of fish production in China. However, during the last decades, with the rapid economic development and population growth in the watershed and neighbor regions, the lake receives an increased loading of PAHs (Xu et al., 2011). The lake with total area of 366 km^2 is composed of 134 interconnected small lakes with different size areas. Lake

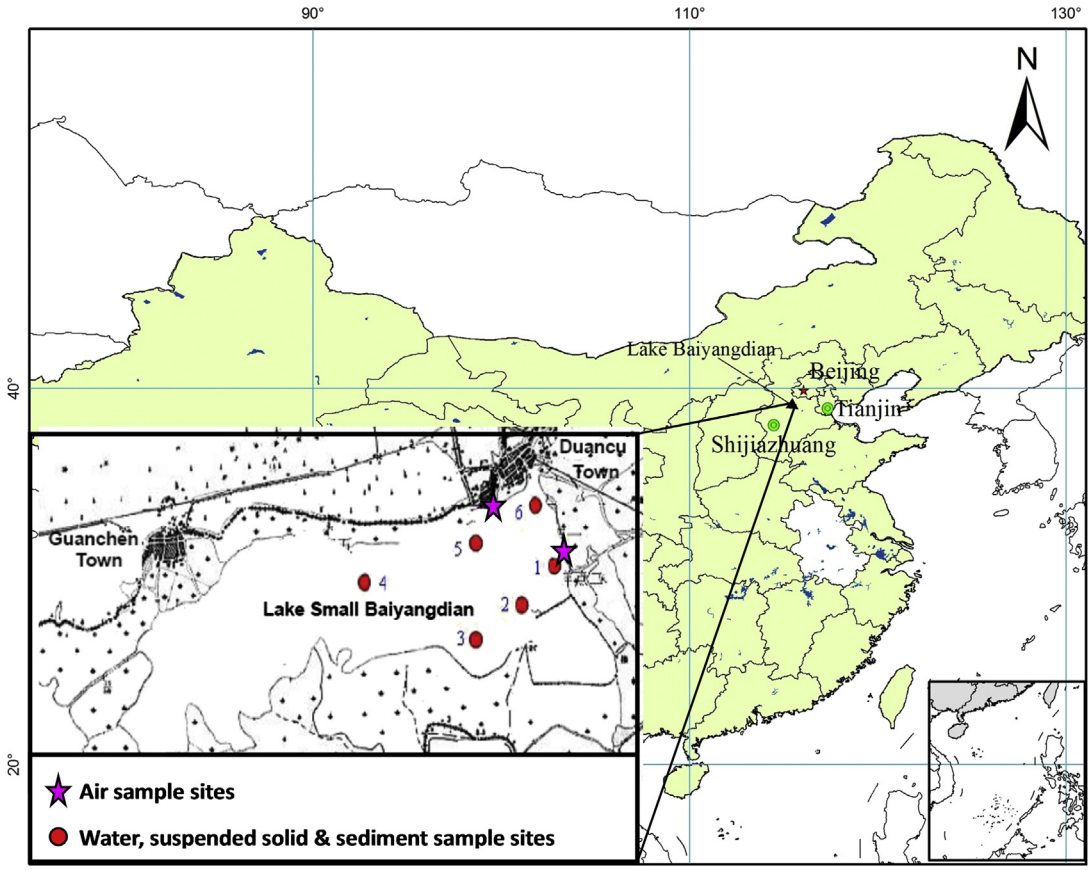

FIGURE 9.1 Location of Lake Small Baiyangdian and sampling sites.

Small Baiyangdian, with the area of 13.3 km^2, is the biggest one among 134 interconnected small lakes.

Sampling for water, suspended solids, sediment, and macrophytes at six sites (Fig. 9.1), and for fish at one site in Lake Small Baiyangdian was performed once on October 7, 2007. Air sampling including gaseous, particulate, and dust samples at two sites was carried out four times seasonally during autumn 2007 to summer 2008. Gaseous and particulate samples were collected using passive air sampler (Tao et al., 2009). Dust samples were collected by dust tank. Macrophytes samples included two species of floating plants, three species of submerged plants, and three species of emergent plant. Four species of commonly consumed freshwater fish including 15 individuals of crucian carp, and 10 individuals each of snakehead fish, grass carp, and silver fish were collected. Fifteen priority PAHs included acenaphthylene (Acy), acenaphthene (Ace), fluorene (Flo), Phe, anthracene (Ant), fluoranthene (Fla), pyrene (Pyr), chrysene (Chr), benzo[a]anthracene (BaA), benzo[b]fluoranthene (BbF), benzo [k]fluoranthene (BkF), BaP, indeno[1,2,3-cd]pyrene (IcdP), benzo[ghi]perylene (BghiP), and

dibenz[a,h]anthracene (DahA) and were measured by GC−MS. Organic carbon contents in water, suspended solids, and sediments, and lipid contents in fish and macrophytes were also analyzed. The mean contents of PAHs, lipid, and organic carbon in the studied multimedia were calculated for the parameters and calibrated for the model.

9.2.3 Model Development

9.2.3.1 Conceptual Framework

A QWASI fugacity model was developed to characterize the multimedia fate of PAHs in Lake Small Baiyangdian. The conceptual diagram of the model is presented in Fig. 9.2. Air, water, and sediment were defined as three bulk compartments. Eight subcompartments included in the three bulk compartments are as follows: air and particles in air; water, suspended solids, plants, and fish in water; and water and solids in sediment. The processes taken into consideration are defined in Fig. 9.2 and additional details are given in Table 9.1.

9.2.3.2 Model Equations

The mass balance equations with fugacities as variables for air, water, and sediment bulk compartments are tabulated in Table 9.2. The equations for the transfer rate coefficients of the modeled processes and for the fugacity capacity of each bulk phase and subphase are listed in Tables 9.3 and 9.4.

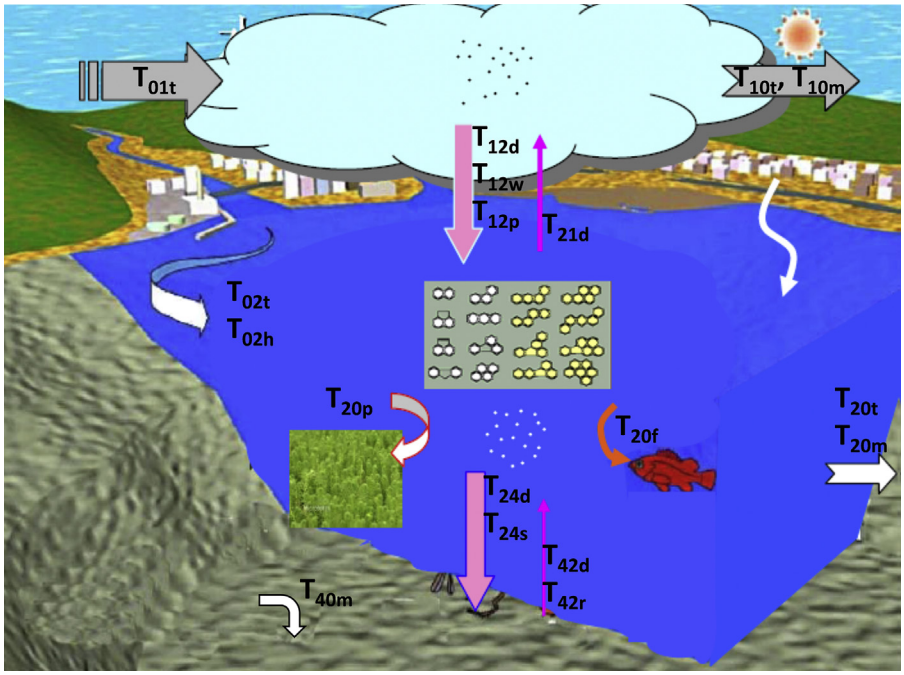

FIGURE 9.2 Conceptual diagram of the QWASI fugacity model for modeling multimedia fates of PAHs in Lake Small Baiyangdian.

TABLE 9.1 Transfer and Transformation Processes Defined in the QWASI Fugacity Model

Symbol	Transfer Process
T_{01t}, T_{10t}	Advective air flows into/out of the lake air bulk
T_{02t}, T_{20t}	Advective water flows into/out of the lake water bulk
T_{02h}	Local wastewater discharge to the lake water bulk
T_{10m}, T_{20m}, T_{40m}	Degradation in air, water, and sediment
T_{20p}, T_{20f}	Bioaccumulation in aquatic plants and fishes
T_{12d}, T_{12p}, T_{12w}	Diffusion, dry deposition, and wet precipitation from air to water
T_{21d}	Diffusion from water to air
T_{24d}, T_{42d}	Diffusion between water column and bottom sediment
T_{24s}	Sedimentation from column and bottom sediment

TABLE 9.2 Mass Balance Equations in the QWASI Fugacity Model

Phase	Mass Balance Equation[a]	Mass Balance Equation in Detail[a]
Air	$T_{01t} + T_{21d} = T_{10t} + T_{10m} + T_{12d} + T_{12p} + T_{12w}$	$Q_{01t}C_{01t} + D_{21d}f_2 = (D_{10t} + D_{10m} + D_{12d} + D_{12p} + D_{12w})f_1$
Water	$T_{02t} + T_{02h} + T_{12d} + T_{12p} + T_{12w} + T_{42d} = T_{20t} + T_{20m} + T_{20f} + T_{20r} + T_{21d} + T_{24d} + T_{24s}$	$Q_{02t}C_{02t} + Q_{02h}C_{02h} + (D_{12d} + D_{12p} + D_{12w})f_1 + D_{42d}f_4 = (D_{20t} + D_{20m} + D_{20f} + D_{20r} + D_{21d} + D_{24d} + D_{24s})f_2$
Sediment	$T_{24d} + T_{24s} = T_{42d} + T_{40m}$	$(D_{24d} + D_{24s})f_2 = (D_{42d} + D_{40m})f_4$

[a] *T_{ijk} are transfer processes, defined in Table 9.1. D_{ijk} are transfer rate coefficients for major transfer processes from the ith bulk phase to the jth bulk phase (see Table 9.3 for details). For system input, $T_{01t} = Q_{01t} \times C_{01t}$, $T_{02t} = Q_{02t} \times C_{02t}$, $T_{02h} = Q_{02h} \times C_{02h}$. For system output, $T_{10t} = D_{10t} \times f_1$, $T_{20t} = D_{20t} \times f_2$, $T_{10m} = D_{10m} \times f_1$, $T_{20m} = D_{20m} \times f_2$, $T_{40m} = D_{40m} \times f_4$, $T_{20p} = D_{20r} \times f_2$, $T_{20f} = D_{2f} \times f_2$. For air–water transfer, $T_{12d} = D_{12d} \times f_1$, $T_{21d} = D_{21d} \times f_2$, $T_{12p} = D_{12p} \times f_1$, $T_{12w} = D_{12w} \times f_1$. For water–sediment transfer, $T_{24d} = D_{24d} \times f_2$, $T_{42d} = D_{42d} \times f_4$, $T_{24s} = D_{24s} \times f_2$.*

9.2.3.3 *Model Parameters*

The model parameters including environmental, physical, chemical, and process kinetic ones were determined in three different ways, i.e. literature review, laboratory experiments, and model calibration. The symbols, descriptions, values, and sources of all model parameters are presented in Tables 9.5 and 9.6. The mean values of collected data are used for the parameters after abnormal values are excluded. The Henry's law constant, saturation vapor pressure and fugacity ratio is the value under the temperature of 25°C. However, the average annual temperature in Lake Small Baiyangdian is 12.1°C. The necessary corrections for these parameters are performed by the Paasivirta's equation (Paasivirta et al., 1999).

TABLE 9.3 Equations for Calculating Transfer Rate Coefficients (D)

Process		Equations[a]	Remarks
Air(1)− water(2)	Diffusion	$D_{12d} = A_2/[1/(K_{12} \times Z_{11}) + 1/(K_{21} \times Z_{22})]$	$D_{21d} = D_{12d}$
	Dry deposition	$D_{12p} = A_2 \times K_p \times X_{13} \times Z_{13}$	
	Wet precipitation	$D_{12w} = A_2 \times K_w \times S_c \times X_{13} \times Z_{13}$	
Water(2) −sediment(4)	Diffusion	$D_{24d} = A_2/[1/(K_{24} \times Z_{22}) + L_4/(B_4 \times Z_{22})]$;	$D_{42d} = D_{24d}$
	Deposition	$D_{24s} = A_2 \times K_s \times Z_{23}$	
Reaction	Degradation in air	$D_{10m} = K_{m1} \times A_1 \times h_1 \times Z_1$	−
	Degradation in water	$D_{20m} = K_{m2} \times A_2 \times h_2 \times (Z_{22} + Z_{23})$	
	Degradation in sediment	$D_{40m} = K_{m4} \times A_4 \times h_4 \times Z_4$	
Advection	Advective air flows	$D_{01t} = Q_{01t} \times Z_1$	−
	Advective water flows	$D_{02t} = Q_{02t} \times Z_2$	
Biota	Fish harvest	$D_{20f} = Y_f \times Z_{2f}/\rho_{2f}$	−
	Plants harvest	$D_{20p} = Y_p \times Z_{2p}/\rho_{2p}$	

[a] *D_{ijk} are transfer rate coefficients for major transfer processes from the ith bulk phase to the jth bulk phase (1, 2, and 4 for air, water, and sediment, respectively, 0 for outside of the area). The subscript k indicates process category (t, d, p, w, f, r, s, and m for advective flow, diffusion, dry deposition, wet precipitation, fish bioaccumulation, pant bioaccumulation, sedimentation, and degradation, respectively). Z is fugacity capacity (see Table 9.4 for details). See Table 9.5 for the meanings of other parameters.*

TABLE 9.4 Equations for Calculating Fugacity Capacities (Z)

Bulk Phase	Subphase	Equations for Calculating Z ($mol/m^3 \cdot Pa$)[a]	
Air	Air	$Z_{11} = 1/RT$	$Z_1 = X_{11}Z_{11} + X_{13}Z_{13}$
	Particle	$Z_{13} = 6E6/(P_S RT)/BP_S$	
Water	Water	$Z_{22} = 1/H$	$Z_2 = X_{22}Z_{22} + X_{23}Z_{23} + X_{2f}Z_{2f} + X_{2p}Z_{2p}$
	Suspended solids	$Z_{23} = O_{23}\rho_{23}K_{oc}/H$	
	Fish	$Z_{2f} = BCF_f/H$	
	Plant	$Z_{2p} = BCF_p/H$	
Sediment	Pore water	$Z_{42} = 1/H$	$Z_4 = X_{42}Z_{42} + X_{43}Z_{43}$
	Solids	$Z_{43} = O_{43}\rho_{43}K_{oc}/H$	

[a] *Z_1, Z_2, and Z_4 are fugacity capacity for air, water, and sediment bulk compartments, respectively. Z_{11}, Z_{13}, Z_{22}, Z_{23}, Z_{2f}, Z_{2p}, Z_{42}, and Z_{43} are fugacity capacity for air and particle subphases in air, water, suspended solids, fish, plant subphases in water, pore water, and solids subphases in sediment, respectively. See Table 9.5 for the meanings of other parameters.*

TABLE 9.5 Parameters for the QWASI Fugacity Model

Symbol	Unit	Parameters	Value	References
A_1, A_2, A_4	m^2	Interface areas of air–water and water–sediment	1.366×10^7	Zhao et al. (2007)
h_1	m	Thickness of air	7.00×10^2	HPEPB (2001) and Ma et al. (2007)
h_2	m	Thickness of water	1.87	HPEPB (2001) and Ma et al. (2007)
h_4	m	Thickness of sediment	1.00×10^{-1}	HPEPB (2001) and Ma et al. (2007)
X_{13}	v/v	Volume fractions of solids in air	9.84×10^{-11}	Mackay and Paterson (1991), note A
X_{23}	v/v	Volume fractions of solids in water	4.29×10^{-6}	Mackay and Paterson (1991), note A
X_{43}	v/v	Volume fractions of solids in sediment	3.00×10^{-1}	Mackay and Paterson (1991), note A
L4	m	Diffusion path lengths in sediment	5.00×10^{-3}	Mackay and Paterson (1991)
X_{2f}	v/v	Volume fractions of fish in water	4.08×10^{-5}	Zhao et al. (2005) and Zhao (1995)
X_{2p}	v/v	Volume fractions of plants in water	8.20×10^{-4}	Zhao et al. (2005) and Zhao (1995)
X_{42}	v/v	Volume fractions of water in sediment	7.00×10^{-1}	Mackay and Paterson (1991)
O_{23}	%	Contents of organic carbon in solids in water	4.41×10^{-1}	Note A
O_{43}	%	Contents of organic carbon in solids in sediment	2.89×10^{-2}	Note A
ρ_{23}	t/m^3	Densities of solids in water	1.89	Note A
ρ_{43}	t/m^3	Densities of solids in sediment	2.49	Note A
ρ_{2f}	t/m^3	Densities of fish in water	1.05	Davenport (1999), note A
ρ_{2p}	t/m^3	Densities of plants in water	8.83×10^{-1}	Davenport (1999), note A
Q_{01t}	m^3/h	Air advection flow into the lake area	1.13×10^{10}	HPEPB (2001), calculated
Q_{10t}	m^3/h	Air advection flow out of the lake area	1.13×10^{10}	HPEPB (2001), calculated
Q_{02t}	m^3/h	Water advection flow into the lake	3.00×10^4	Yin (2008)
Q_{20t}	m^3/h	Water advection flow out of the lake	2.50×10^4	Yin (2008)
Q_{02h}	m^3/h	Rate of local wastewater discharge	500	HPEPB (2001), calculated

(*Continued*)

TABLE 9.5 Parameters for the QWASI Fugacity Model—cont'd

Symbol	Unit	Parameters	Value	References
C_{02t}	mol/m^3	PAHs concentration in water advection flow	Note B	Bai (2008), note A
C_{02h}	mol/m^3	PAHs concentration in wastewater	Note B	Note A
Y_f	T/h	Harvest rate of fish	3.00	Zhao et al. (2005) and Zhao (1995)
Y_P	T/h	Harvest rate of plants	6.00×10^1	Zhao et al. (2005) and Zhao (1995)
T	K	Local average temperature	3.00×10^2	Zhao et al. (2007)
Ps_{25}	Pa	Local vapor pressure	Note B	Van Agreren et al. (1998), Mackay et al. (1997), Wang (1991), Wang (1993), and Jin (1990)
R	$Pa \cdot m^3/mol \cdot K$	The gas constant	8.314	Van Agreren et al. (1998), Mackay et al. (1997), and Karickhoff (1981)
F_{25}	–	Fugacity ratio at 25°C	Note B	Mackay et al. (1997)
H_{25}	$Pa \cdot m^3/mol$	Henry's constant	Note B	Mackay et al. (1997), Wang (1991), Wang (1993), Jin (1990), and Ten Hulscher et al. (1992)
B_F	–	Fugacity ratio temperature correction factor	Note B	Paasivirta et al. (1999)
B_H	–	Henry's law constant temperature correction factor	Note B	Paasivirta et al. (1999)
BP_S	–	Saturation vapor pressure temperature correction factor	Note B	Paasivirta et al. (1999)
K_{oc}	m^3/t, 1/h	Adsorption coefficient	Note B	Mackay et al. (1997), Jin (1990), STF (1991), and US-EPA (1996)
K_{m1}	1/h	Degradation rate of PAHs in air	Note B	Mackay (2001) and Lang et al. (2008)
K_{m2}	1/h	Degradation rate of PAHs in water	Note B	Mackay (2001) and Lang et al. (2008)
K_{m4}	1/h	Degradation rate of PAHs in sediment	Note B	Mackay (2001), Lang et al. (2008)
BCF_f	m^3/t	Bioconcentration factor of fish	Note B	Lang et al. (2008), Duan (2005), and Tang et al. (2006), note A (calculated)
BCF_p	m^3/t	Bioconcentration factor of plants	Note B	Lang et al. (2008), Duan (2005), and Tang et al. (2006), note A (calculated)
B_1	m^2/h	Molecular diffusivities in air	Note B	Perry and Chilton (1973), US-EPA (1996), Shor et al. (2003), and Xu (1991)

(*Continued*)

TABLE 9.5 Parameters for the QWASI Fugacity Model—cont'd

Symbol	Unit	Parameters	Value	References
B_2	m^2/h	Molecular diffusivities in water	Note B	Perry and Chilton (1973); US-EPA (1996), Shor et al. (2003), and Xu (1991)
B_4	m^2/h	Molecular diffusivities in sediment	Note B	Perry and Chilton (1973), US-EPA (1996), Shor et al. (2003), and Xu (1991)
K_{12}	m/h	Air-side molecular transfer coefficient over water	3.00	Thibodeaux (1996) and Banks and Herrera (1997)
K_{21}	m/h	Water-side molecular transfer coefficient over air	3.00×10^{-2}	Thibodeaux (1996), Banks and Herrera (1997)
K_{24}	m/h	Water-side molecular transfer coefficient over sediment	1.00×10^{-2}	Thibodeaux (1996) and Banks and Herrera (1997)
K_P	m/h	Dry deposition velocity	5.69×10^{-1}	HPEPB (2001), Mackay and Paterson (1991), Beijing Statistics Bureau (2005), and Tainjin Environment Protection Bureau (1991, 1996, 2001)
K_w	m/h	Wet deposition velocity	6.51×10^{-5}	HPEPB (2001), Mackay and Paterson (1991), Beijing Statistics Bureau (2005), and Tainjin Environment Protection Bureau (1991, 1996, 2001)
K_S	m/h	Water sedimentation rates	4.60×10^{-6}	Chen et al. (2006) and Hu et al. (1998)
S_C	m/h	Rain scavenging rate	2.00×10^{5}	Mackay et al. (1986)

Note A: Data determined in our lab.
Note B: Presented in Table 9.6.

9.2.3.4 Multimedia Modeling

The concentrations of PAHs in the compartments and the transfer fluxes between adjacent compartments were modeled under a steady-state assumption. Measured concentrations in this study were used for model validation. Modeling was performed using Matlab v.6.5 (MathWorks, 2002). SPSS v.10.0 and MS Excel were employed for statistical analysis and data manipulation.

9.2.3.5 Sensitivity Analysis

An overview of the most sensitive components of the model can be determined through sensitivity analysis. This analysis provides a measure of the sensitivity of parameters, forcing functions or submodels to the state variables of greatest interest in the model. In practical modeling, the sensitivity analysis is carried out by changing the parameters, forcing functions and submodels, and the corresponding response of the selected state variables is observed (Jørgensen and Nielsen, 1994). In this study, the sensitivity analysis was performed

TABLE 9.6 Parameter Values for Different PAH Components in the QWASI Fugacity Model

Symbols	ACE	ACY	FlO	PHE	ANT	FLA	PYR	BaA	CHR	BbF	BkF	BaP	DahA	IcdP	BghiP
C_{01t}	5.27E-11	1.90E-11	3.31E-10	5.80E-10	2.61E-11	1.27E-10	6.48E-11	9.96E-12	1.18E-10	8.81E-11	5.83E-12	2.25E-11	1.93E-11	1.05E-11	3.64E-11
C_{02t}	1.71E-08	1.30E-08	4.21E-08	4.49E-08	6.17E-08	2.37E-08	1.14E-08	1.31E-09	4.38E-09	1.19E-09	7.930E-10	3.96E-10	1.09E-09	1.08E-09	0.00E+00
C_{02h}	8.35E-07	7.33E-07	1.88E-06	1.63E-06	3.69E-06	1.40E-06	5.93E-07	7.64E-08	2.51E-07	6.53E-08	4.71E-08	1.64E-08	6.38E-08	2.77E-08	0.00E+00
H_{25}	1.78E+01	1.16E+01	8.50E+00	4.00E+00	6.00E+00	1.49E+00	1.53E+00	8.61E-01	1.83E-01	5.40E-02	8.53E-02	9.00E-03	7.00E-03	7.00E-03	1.00E-03
Ps_{25}	1.31E+00	2.12E+00	4.83E-01	5.98E-02	1.41E-02	2.34E-03	1.91E-03	5.74E-05	2.21E-05	4.45E-06	3.79E-06	3.22E-06	3.22E-06	3.22E-06	3.22E-06
K_{oc}	4.36E+03	6.76E+03	1.08E+04	1.81E+04	6.05E+04	2.41E+05	3.92E+04	4.04E+05	1.68E+06	1.68E+06	2.15E+06	5.25E+05	2.60E+06	4.89E+06	4.89E+06
BCF_f	4.81E+02	4.74E+02	9.65E+02	1.86E+03	1.93E+03	4.75E+03	3.43E+03	3.43E+03	2.02E+04	6.17E+04	7.78E+04	3.86E+04	3.86E+04	3.86E+04	3.86E+04
BCF_v	5.94E+01	8.91E+01	1.04E+02	3.32E+02	9.75E+02	1.00E+03	1.17E+03	7.12E+03	2.99E+03	4.26E+03	6.69E+03	7.33E+03	2.10E+04	3.72E+04	2.10E+04
K_{m1}	5.04E-03	5.04E-03	5.04E-03	5.04E-03	5.04E-03	4.08E-03	4.08E-03	4.08E-03	4.08E-03	4.08E-03	4.08E-03	4.08E-03	4.08E-03	4.08E-03	4.08E-03
K_{m2}	5.04E-04	5.04E-04	5.04E-04	5.04E-04	5.04E-04	4.08E-04	4.08E-04	4.08E-04	4.08E-04	4.08E-04	4.08E-04	4.08E-04	4.08E-04	4.08E-04	4.08E-04
K_{m4}	1.63E-05	1.63E-05	1.63E-05	1.63E-05	1.63E-05	1.26E-05	1.26E-05	1.26E-05	1.26E-05	1.26E-05	1.26E-05	1.26E-05	1.26E-05	1.26E-05	1.26E-05
B_1	1.66E-02	1.80E-02	1.55E-02	1.66E-02	1.47E-02	1.38E-02	1.34E-02	1.55E-02	1.25E-02	1.18E-02	1.18E-02	1.41E-02	1.11E-02	1.10E-02	1.33E-02
B_2	2.17E-06	1.88E-06	2.14E-06	1.85E-06	2.09E-06	1.85E-06	1.96E-06	2.10E-06	1.77E-06	1.64E-06	1.64E-06	2.05E-06	1.55E-06	1.60E-06	1.39E-06
B_4	4.54E-13	4.57E-13	4.37E-13	4.63E-12	7.55E-11	2.21E-11	2.88E-11	7.99E-12	6.87E-12	1.51E-12	1.89E-12	1.58E-12	3.15E-13	2.38E-13	6.26E-13
F_{25}	1.97E-01	3.38E-01	1.39E-01	2.08E-01	1.01E-02	7.62E-02	1.57E-01	5.07E-02	6.68E-03	6.68E-03	1.26E-02	3.11E-03	3.11E-03	3.11E-03	3.11E-03
B_F	1.13E+03	5.73E+02	1.02E+03	8.60E+02	1.51E+03	8.93E+02	9.87E+02	1.12E+03	1.37E+03	9.06E+02	1.45E+03	1.30E+03	9.09E+02	1.29E+03	1.12E+03
B_H	1.24E+03	2.18E+03	1.59E+03	2.12E+03	1.36E+03	2.48E+03	2.34E+03	2.64E+03	2.77E+03	3.56E+03	2.98E+03	3.28E+03	4.01E+03	3.21E+03	3.37E+03
BPs	3.49E+03	3.32E+03	3.64E+03	3.84E+03	4.38E+03	4.26E+03	4.31E+03	4.88E+03	5.51E+03	5.37E+03	5.87E+03	5.82E+03	5.82E+03	5.82E+03	5.82E+03

Note: The meanings of the symbols are the same with them in Table 9.5.

only for the parameters. A change for the parameter at ±10% was chosen, and the sensitivity coefficient (S) was calculated by the following formula (Cao et al., 2004):

$$S = (Y_{1.1} - Y_{0.9})/(0.2 \cdot Y) \quad (12.1)$$

Y represents the model outputs of chemical concentrations. The terms, $Y_{1.1}$ and $Y_{0.9}$, represent the estimated concentrations when the tested parameter was changed at +10% and −10%, respectively. The greater the absolute value of sensitivity coefficient, the more sensitive the parameter.

9.2.3.6 *Uncertainty Analysis*

Both concentrations and fluxes estimated by the multimedia model are inherently variable (McKone, 1996). In addition to the inherent variability, there are also uncertainties in the parameters and estimates (Tao et al., 2003). For assessing the overall uncertainty and variability in predictions, Monte Carlo simulation was used to illustrate collective variance of the inputs through the model. Each input parameter was represented as a probability density function that defined both the range of values and the likelihood of the parameter having that value. All of the parameters were assumed to follow the log-normal distribution. The simulation was undertaken repeatedly 3000 times, with new values randomly selected for all parameters within the range of mean ± standard deviation. A built-in function of "randn" in Matlab was used to select the values randomly for each parameter (MathWorks, 2002). The model uncertainty was ascertained by statistical analysis on the output result. To quantify the differences, coefficients of variation (CVs) were calculated based on log-transformed data.

9.2.4 Results and Discussion

9.2.4.1 *Modeled Concentration Distributions*

The levels and distributions of calculated PAHs concentrations in the three bulk and seven subphases are presented in Table 9.7. The highest PAHs concentrations were found in the sediment phase, followed by the water and air phases (Fig. 9.3). The percentage ratios of individual PAH congeners ranged from 58.9% to 88.5%, 11.5 to 26.8%, and 0 to 14.3% for the sediment, water, and air phases, respectively (Fig. 9.3). This implies that the sediment would serve as the sink of PAHs. Among different PAHs congeners, low-molecular-weight PAHs (LMW-PAHs) predominated the distribution in three bulk phases. From LMW-PAHs to middle- and high-molecular-weight PAHs (MMW-PAHs and HMW-PAHs), the average percentage were increased from 64.8% to 66.1% and 87.0% in the sediment, and decreased from 26.3% to 22.9% and 13.0% in the water, and 11.0 to 8.9% and 0 in the air. This means that LMW-PAHs were in higher proportion in the water and air, while HMW-PAHs were in higher proportion in the sediment.

Fig. 9.4 illustrates that the different distribution patterns of LMW-PAHs, MMW-PAHs, and HMW-PAHs in seven subphases. In the air, LMW-PAHs predominated in the gaseous subphase, while HMW-PAHs were dominant in solid-particle subphase (Fig. 9.4A). In the water, the PAHs contents in subphases were in the declining order of suspended solids (C23) > fish (C2f) > aquatic plants (C2p) > dissolved subphase (C22); and PAHs contents in the dissolved

TABLE 9.7 Calculated PAHs Concentration in the Bulk and Subphases

	C1	C2	C4	C13	C22	C23	C2f	C2p	C42	C43
ACE	5×10^{-11}	5×10^{-9}	5×10^{-5}	1×10^{-14}	5×10^{-9}	2×10^{-5}	2×10^{-6}	3×10^{-7}	5×10^{-7}	2×10^{-4}
ACY	2×10^{-11}	1×10^{-19}	1×10^{-5}	5×10^{-15}	1×10^{-9}	5×10^{-6}	6×10^{-7}	1×10^{-7}	1×10^{-7}	5×10^{-5}
FlO	3×10^{-10}	2×10^{-8}	4×10^{-4}	1×10^{-13}	2×10^{-8}	2×10^{-4}	2×10^{-5}	2×10^{-6}	2×10^{-6}	1×10^{-3}
PHE	6×10^{-10}	3×10^{-8}	9×10^{-4}	3×10^{-12}	2×10^{-8}	3×10^{-4}	4×10^{-5}	7×10^{-6}	2×10^{-6}	3×10^{-3}
ANT	2×10^{-11}	6×10^{-10}	4×10^{-5}	3×10^{-14}	3×10^{-10}	1×10^{-5}	5×10^{-7}	3×10^{-7}	3×10^{-8}	1×10^{-4}
FLA	1×10^{-10}	1×10^{-9}	3×10^{-4}	7×10^{-12}	5×10^{-10}	9×10^{-5}	2×10^{-6}	5×10^{-7}	6×10^{-8}	1×10^{-3}
PYR	6×10^{-11}	4×10^{-9}	2×10^{-4}	8×10^{-12}	2×10^{-9}	6×10^{-5}	6×10^{-6}	2×10^{-6}	3×10^{-7}	7×10^{-4}
BaA	7×10^{-12}	4×10^{-10}	6×10^{-5}	5×10^{-12}	5×10^{-11}	2×10^{-5}	2×10^{-7}	3×10^{-7}	7×10^{-9}	2×10^{-4}
CHR	1×10^{-11}	2×10^{-10}	8×10^{-5}	6×10^{-12}	2×10^{-11}	2×10^{-5}	3×10^{-7}	5×10^{-8}	2×10^{-9}	3×10^{-4}
BbF	1×10^{-11}	3×10^{-10}	1×10^{-4}	1×10^{-11}	2×10^{-11}	3×10^{-5}	2×10^{-6}	1×10^{-7}	3×10^{-9}	4×10^{-4}
BkF	5×10^{-12}	1×10^{-10}	5×10^{-5}	5×10^{-12}	8×10^{-12}	1×10^{-5}	6×10^{-7}	5×10^{-8}	1×10^{-9}	2×10^{-4}
BaP	8×10^{-13}	5×10^{-11}	7×10^{-6}	6×10^{-13}	4×10^{-12}	2×10^{-6}	2×10^{-7}	3×10^{-8}	6×10^{-10}	2×10^{-5}
DahA	1×10^{-12}	3×10^{-11}	9×10^{-6}	8×10^{-13}	1×10^{-12}	2×10^{-6}	4×10^{-8}	2×10^{-8}	2×10^{-10}	3×10^{-5}
IcdP	8×10^{-13}	2×10^{-11}	7×10^{-6}	6×10^{-13}	5×10^{-13}	2×10^{-6}	2×10^{-8}	2×10^{-8}	7×10^{-11}	2×10^{-5}
BghiP	2×10^{-12}	3×10^{-11}	1×10^{-5}	1×10^{-12}	9×10^{-13}	4×10^{-6}	4×10^{-8}	2×10^{-8}	1×10^{-10}	5×10^{-5}

Note: *C1*, air phase; *C2*, water phase; *C4*, sediment phase; *C13*, solid particles in air phase; *C22*, dissolved in water phase; *C23*, solid particles in water phase; *C2f*, fish in water phase; *C2p*, aquatic plants in water phase; *C42*, pore water in sediments; *C43*, solid particles in sediment phase.

phase were much lower than these in the suspended solid, fish, and aquatic plant subphases. From LMW-PAHs to MMW-PAHs and HMW-PAHs, the contents were decreased in the dissolved subphase, and similar in the suspended solids, fish, and plant subphases (Fig. 9.4B). In the sediment, PAHs contents in the solid subphase (C43) were significantly higher than these in pore water subphase (C42) (Fig. 9.4C).

The different fate behaviors of LMW-PAHs, MMW-PAHs, and HMW-PAHs in the water, air, and sediment may be attributed to the difference in their physical and chemical properties. LMW-PAHs with higher vapor pressure and Henry's law constant are more volatile than HMW-PAHs with lower vapor pressure and Henry's law constant. On the other hand, LMW-PAHs are less lipophilic due to their lower K_{oc} values, so that their ability in binding to organic matter in suspended solids and sediments is obviously weaker than that of HMW-PAHs. The dissolved PAHs concentrations in the water and pore water were decreased with the increase of their molecular weight, probably due to the decreasing solubility.

9.2.4.2 Model Validation

The model was validated by the comparisons between calculated and measured PAHs concentrations in the subphases. As can be seen in Fig. 9.5, very similar distribution patterns

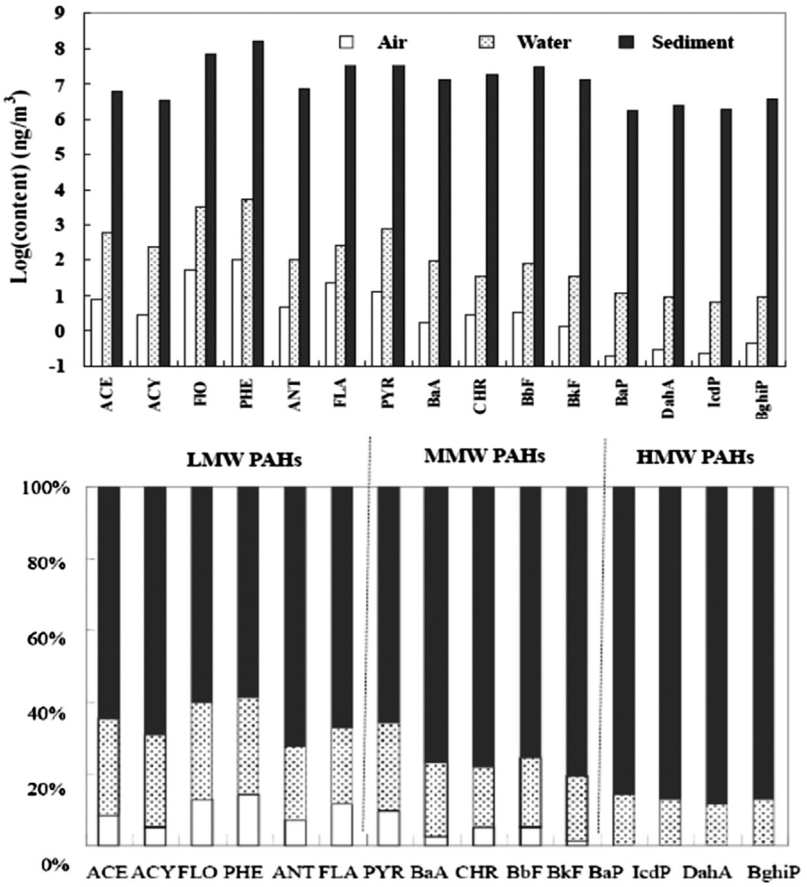

FIGURE 9.3 Distributions of calculated PAHs concentration and their percentage in three bulks.

in the subphases of the water and sediment would be found in both calculated and measured PAHs concentrations. The simulated values for the most of PAHs congeners were lower than their measured values, which may be attributed to the neglect of some input process such as soil erosion. The difference between the calculated and measured PAHs concentrations were different for both the subphases and PAH congeners. Among seven subphases, the best agreements with the difference less than one order of magnitude could be found for the PAHs concentrations in the solid subphase in the sediment (C43), while the worst agreements with the difference around two orders of magnitude were for the PAHs concentrations in the dissolved and solid subphase in water (C22 and C23). Among 15 PAH congeners, LMW-PAHs maintain better agreements in all subphases than HMW-PAHs. The best agreements with the difference less than one order of magnitude could be found for the LMW-PAHs except for Acy and ANT in the suspended solid subphases (C23) and ANT in

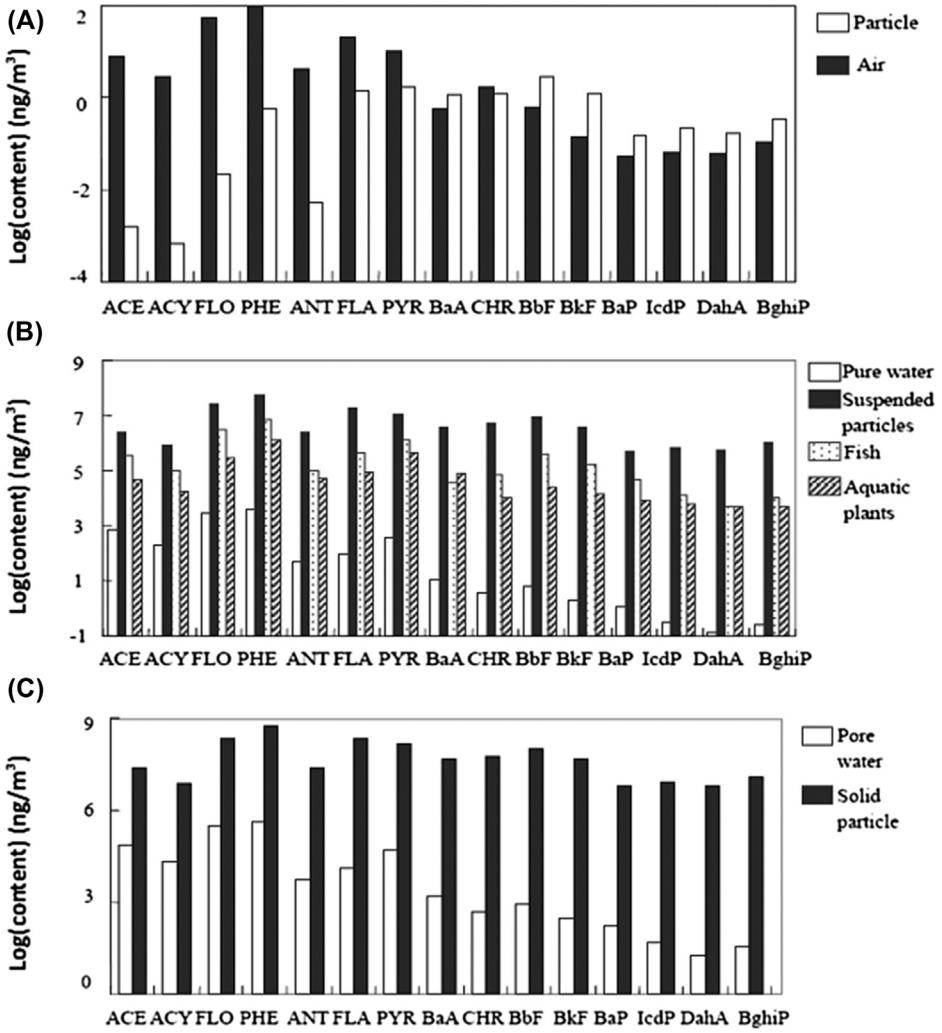

FIGURE 9.4 Calculated PAHs concentrations in the subphases in Lake Small Baiyangdian.

the fish subphases (C2f). The worst agreements with the difference around two orders of magnitude were for the HMW-PAHs in the suspended solid and fish subphases (C23 and C2f). The IcdP and DahA in the suspended solid and fish subphases as well as the BghiP in the suspended solid subphase were undetectable; however, their modeled values were relatively high.

The differences between the calculated and measured PAHs concentrations for seven subphases are attributable to the complexity of PAHs sources and the degree of influence by environmental changes; however, those for PAH congeners are attributed to their

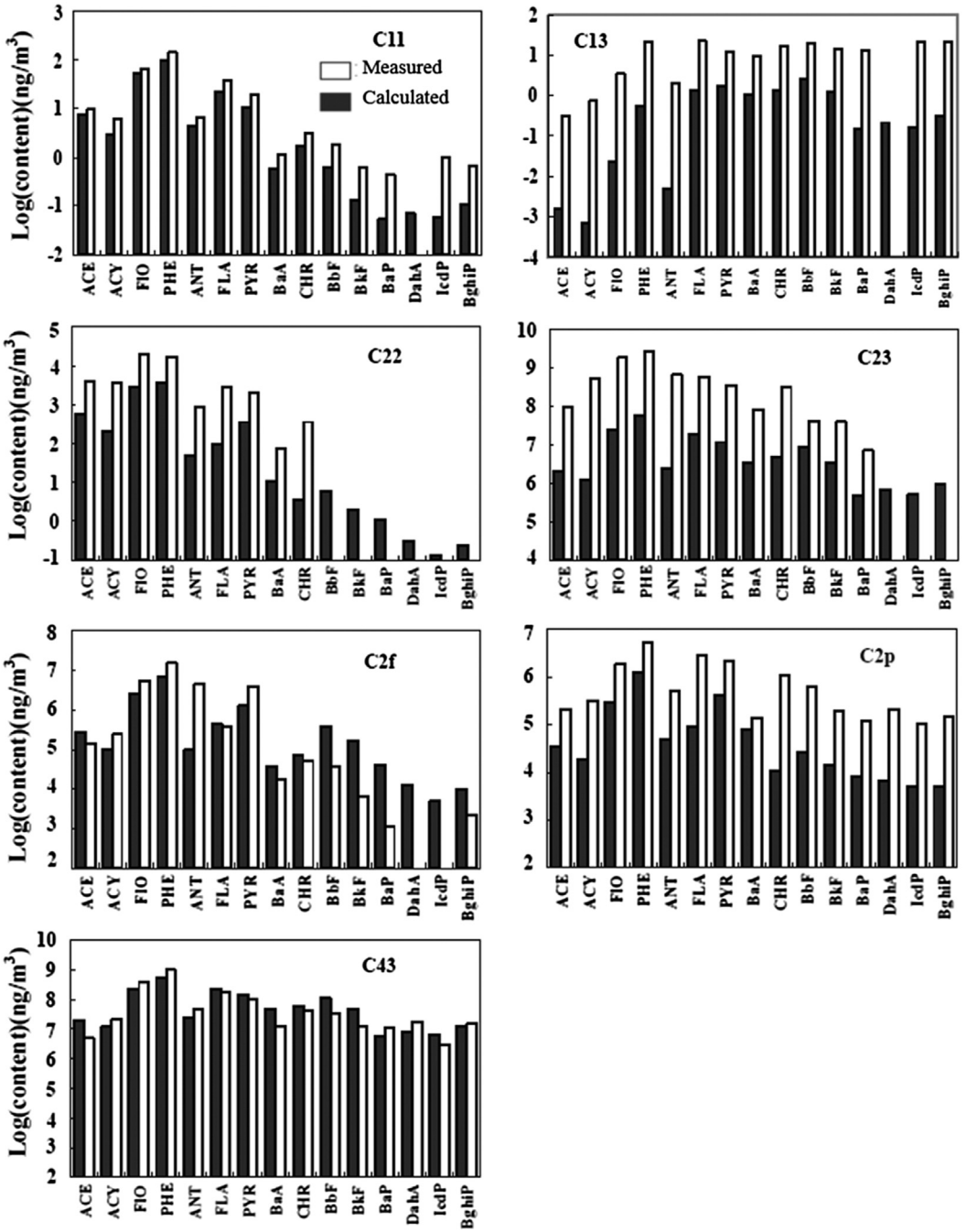

FIGURE 9.5 Comparisons between the calculated and measured concentration of PAHs in seven subphases.

different physical and chemical properties. The PAHs in the solid subphase in sediment were mainly from the sedimentation of suspended solids in water and were less influenced by ambient environmental changes. However, the PAHs in the dissolved and solid subphase in water were likely from the input of inflow rivers, surface runoff, dry and wet depositions, and they were easily influenced by ambient environmental changes. Compared with the concentrations of LMW-PAHs, the HMW-PAHs are much lower in concentration and are often undetectable or with large uncertainty (see Section 9.2.3.6 for details).

9.2.4.3 Transfer Fluxes of PAHs

The calculated transfer fluxes of PAHs are shown in Table 9.8. The fluxes into and out of the lake area as well as each compartment were well balanced. For instance, for the total flux into and out of the lake area, the average and maximum relative errors were 0.022% and 0.19% (Ant), respectively. The fluxes through advective air flows into and out of the lake (T_{01t}, T_{10t}) were predominant in the input and output fluxes of PAHs. The average bioaccumulation flux of 15 PAHs by plants (T_{2p}) was four times higher than that by fish (T_{2f}). The highest percentage of the average flux of 15 PAHs by degradation in the sediment (T_{40m}) was 61.81%, followed by the air (T_{10m}) (37.82%) and by the water (T_{20m}) (0.37%). From LMW-PAHs to MMW-PAHs and HMW-PAHs, the percentages of the average flux by degradation in the sediment (T_{40m}) were increased from 42.70% to 74.32% and 79.15%; however, those by degradation in the air (T_{10m}) were decreased from 56.60% to 25.56% and 20.78%. This meant that the degradation of LMW-PAHs mainly occurred in the air and that the degradation of MMW-PAHs and HMW-PAHs mainly happened in the sediment.

The calculated transfer fluxes of PAHs across the air−water and water−sediment interfaces are shown in Fig. 9.6. The transfer fluxes from air to water across the air−water interface and from water to sediment across the water−sediment interface were much higher than these from water to air and from sediment to water, respectively. This indicated that, in the air−water−sediment system, the transfer directions of PAHs were from air to water and to sediment. Air was the source of PAHs, while sediment could severe as the sink of PAHs. Among 15 PAH congeners, the highest transfer fluxes from air to water (T_{12}) and from water to sediment (T_{24}) could be found for LMW-PAHs (including 2- and 3-ring PAHs), followed by MMW-PAHs and HMW-PAHs.

Fig. 9.7 illustrates that contributions of the transfer fluxes of PAHs from air to water and from water to sediment though different processes were changed. From air to water (Fig. 9.7A), the transfer of LMW-PAHs by the diffuse process (T_{12d}) contributed the highest fluxes, followed by wet and dry precipitation processes (T_{12p} and T_{12w}). For MMW-PAHs and HMW-PAHs, the wet precipitation played the highest contribution of transfer fluxes (T_{12w}), followed by the diffuse and dry precipitation (T_{12d} and T_{12p}). From LMW-PAHs (including 2- and 3-ring PAHs) to MMW-PAHs and HMW-PAHs, the transfer fluxes through diffuse process (T_{12d}) were decreased. The transfer fluxes through dry and wet precipitations (T_{12p} and T_{12w}) were increased from 2-ring PAHs to 3- and 4-ring PAHs. From water to sediment (Fig. 9.7B), the transfer fluxes of PAHs were mainly depended on the sedimentation process (T_{24s}). The diffuse process (T_{24d}) could only have some contributions for 2-, 3-, and 4-ring PAHs.

TABLE 9.8 Calculated Transfer Fluxes In and Out of the Lake Area As Well As Each Compartment

	T_{01t}	T_{02t}	T_{02h}	T_{10t}	T_{20t}	T_{12d}	T_{12p}	T_{12w}	T_{21d}	T_{24d}	T_{24s}	T_{42d}	T_{10m}	T_{20m}	T_{40m}	T_{2p}	T_{2f}
ACE	3.74E+00	5.12E-04	4.17E-04	3.65E+00	9.51E-05	3.80E-02	2.16E-06	4.95E-05	1.36E-02	1.26E-10	2.32E-02	1.36E-08	6.64E-02	1.33E-03	2.32E-02	1.44E-05	5.77E-06
ACY	1.35E+00	3.89E-04	3.67E-04	1.31E+00	2.24E-05	1.66E-02	9.46E-07	2.17E-05	2.84E-03	4.68E-11	1.33E-02	5.07E-09	2.39E-02	4.94E-04	1.33E-02	7.97E-06	2.10E-06
FlO	2.35E+01	1.26E-03	9.38E-04	2.28E+01	3.25E-04	2.93E-01	2.83E-05	6.48E-04	3.15E-02	5.40E-10	2.56E-01	5.86E-08	4.15E-01	6.04E-03	2.56E-01	1.12E-04	5.16E-05
PHE	4.12E+01	1.35E-04	8.16E-04	3.99E+01	5.31E-04	5.65E-01	6.73E-04	1.54E-02	1.78E-02	7.41E-09	5.55E-01	8.05E-07	7.22E-01	8.02E-03	5.55E-01	4.64E-04	1.29E-04
ANT	1.86E+00	1.85E-03	1.84E-03	1.80E+00	6.79E-06	2.36E-02	5.98E-06	1.37E-04	4.10E-04	1.52E-09	2.34E-02	1.66E-07	3.22E-02	1.16E-04	2.34E-02	1.72E-05	1.69E-06
FLA	9.05E+00	7.12E-04	6.99E-04	8.77E+00	1.31E-05	1.20E-01	1.46E-03	3.33E-02	1.28E-04	7.38E-10	1.54E-01	1.04E-07	1.24E-01	2.37E-04	1.54E-01	2.92E-05	6.87E-06
PYR	4.60E+00	3.41E-04	2.96E-04	4.43E+00	4.48E-05	5.77E-02	1.74E-03	3.99E-02	5.39E-04	3.76E-09	9.81E-02	5.29E-07	6.52E-02	5.68E-04	9.81E-02	1.33E-04	1.94E-05
BaA	5.65E-01	3.94E-05	3.82E-05	5.30E-01	1.20E-06	2.73E-03	1.02E-03	2.33E-02	7.40E-06	2.79E-11	2.70E-02	3.93E-09	7.76E-03	3.26E-05	2.70E-02	2.17E-05	5.19E-07
CHR	8.36E+00	1.31E-04	1.26E-04	8.31E+00	5.86E-06	8.16E-03	1.18E-03	2.70E-02	4.91E-07	7.75E-12	3.63E-02	1.09E-09	1.37E-02	3.01E-05	3.63E-02	2.95E-06	9.87E-07
BbF	6.26E+00	3.57E-05	3.26E-05	6.18E+00	3.04E-06	2.84E-03	2.28E-03	5.23E-02	1.74E-07	2.69E-12	5.73E-02	3.79E-10	1.42E-02	4.76E-05	5.73E-02	6.63E-06	4.76E-06
BkF	4.14E-01	2.38E-05	2.36E-05	3.84E-01	2.06E-07	5.75E-04	1.01E-03	2.31E-02	1.13E-07	1.13E-12	2.46E-02	1.59E-10	5.61E-03	1.98E-05	2.46E-02	3.49E-06	2.01E-06
BaP	1.60E+00	1.19E-05	8.19E-06	1.59E+00	3.70E-06	2.36E-04	1.24E-04	2.85E-03	5.71E-09	5.03E-13	3.20E-03	7.09E-11	8.49E-04	3.49E-06	3.20E-03	2.04E-06	5.32E-07
DahA	1.37E+00	3.26E-05	3.19E-05	1.36E+00	6.47E-07	2.71E-04	1.64E-04	3.75E-03	9.06E-10	2.65E-14	4.19E-03	3.73E-12	1.08E-03	3.30E-06	4.19E-03	1.54E-06	1.41E-07
IcdP	7.45E-01	3.23E-05	1.38E-05	7.41E-01	1.85E-05	2.36E-04	1.25E-04	2.86E-03	4.91E-10	8.17E-15	3.22E-03	1.15E-12	8.52E-04	2.42E-06	3.22E-03	1.12E-06	5.74E-08
BghiP	2.58E+00	0	5.89E-07	2.57E+00	5.89E-07	4.35E-04	2.44E-04	5.59E-03	1.29E-10	4.18E-14	6.26E-03	5.89E-12	1.64E-03	4.71E-06	6.26E-03	1.23E-06	1.12E-07

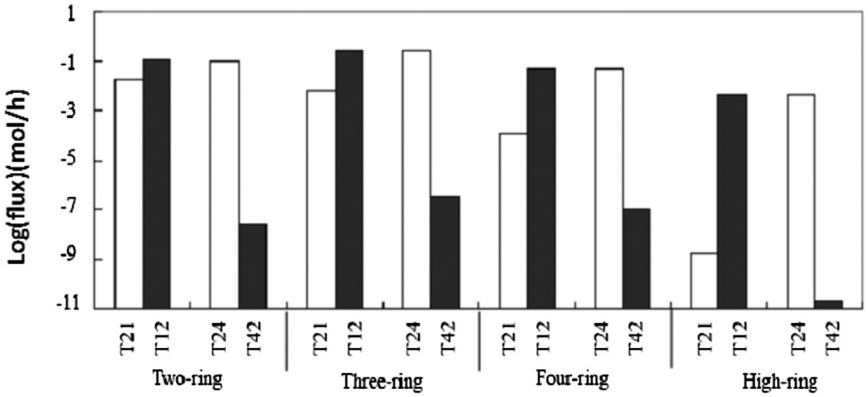

FIGURE 9.6 Transfer fluxes of PAHs across the air–water and water–sediment interfaces in Lake Small Baiyangdian.

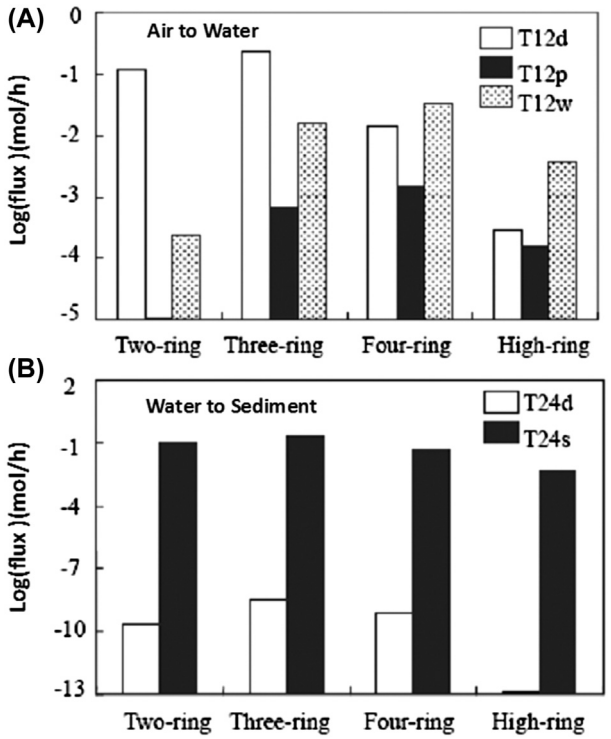

FIGURE 9.7 Transfer fluxes of PAHs through different processes from air to water (A) and from water to sediment (B) in Lake Small Baiyangdian.

9.2.4.4 Sensitivities of Modeled Concentrations to Input Parameters

The parameters with sensitivity coefficients higher than 0.5 are considered as more influential parameters in the model. Four compounds, Ace, Phe, Chr, and BaP, were chosen to represent 2-, 3-, 4-, and high-ring PAHs. The model outputs included the concentrations of four representative PAH compounds in the four subphases in the water including dissolved phase (C22), suspended solids (C23), fish (C2f), and aquatic plants (C2p), and in solids subphase in the sediment (C43). The results were summarized in Table 9.9. Among 54 parameters, there were only 17 parameters with sensitivity coefficients higher than 0.5. Temperature (T) was the most influential parameter in the model, and was more sensitive to the model concentrations for Chr and BaP than those for Ace and Phe in all the studied subphases (C22, C23, C2f, C2p, and C43). The number of sensitive parameters for BaP in the studied subphases was 9–13, however, that for Ace and Phe was only three to seven. There were only three parameters, T, K_s, and K_{12}, sensitive to Ace and Phe in C23. For the modeled concentration in a specific studied subphase, the parameters for BaP and Chr were more sensitive than those for Ace and Phe.

9.2.4.5 Uncertainty of the Modeled Concentrations

3000 Monte Carlo simulations were performed to simulate the concentrations of four representative PAHs (Ace, Phe, Chr, and BaP) in the seven subphases. Coefficients of variation (CVs) for Ace, Phe, Chr, and BaP in the seven subphases are shown in Fig. 9.8 and the heights of the bars indicate the perturbations of the calculated concentrations.

Fig. 9.8 illustrates that, among four representative PAH components, BaP had the highest CV values of 29% in the particulate subphase in air (C13) to 50% in the sediments (C43), followed by Chr with the CV ranging from about 4% in the particulate subphase in the air (C13) to 22% in the plant subphase in the water (C2p); however, all the CV values for Ace and Phe in seven subphases were less than 5%. This indicated that there were the highest uncertainty for the modeled BaP concentration, and very low uncertainty for the modeled Ace and Phe concentrations. In seven subphases studied, the variabilities for the modeled Ace and Phe concentrations were relatively similar to each other, and those for the modeled Chr and BaP concentrations were in a descending order of $C2p > C22 \approx C2f > C43 \approx C11 > C23 \approx C13$, and of $C43 > C2f > C23 \approx C22 > C11 > C2p \approx C13$, respectively. The largest uncertainties of the calculated BaP concentrations are related to the most influential parameters identified in the sensitivity analysis (Table 9.9).

9.2.5 The Ecological Implications of the Proposed Model

Ecotoxicological models are increasingly applied to assess the fate and effect of chemical emissions to the environment, and they can be divided into three types, fate models, effect models, and fate-transport-effect models (FTE models; Jørgensen and Fath, 2011). Fate models provide the concentration of a chemical in one or more environmental compartments; effect models translate a concentration or body burden in a biological compartment to an effect either on an organism, a population, a community, an ecosystem, a landscape, or the entire ecosphere; and fate-transport-effect models are the merging of fate models with effect models (Jørgensen and Fath, 2011). So far, many fate models, fewer effect models, and only a

TABLE 9.9 Sensitivity Coefficients of the More Sensitive Parameters in the QWASI Fugacity Model (SCi > 0.5)

		X_{13}	X_{43}	r_{23}	K_{12}	h_4	O_{23}	T	K_s	Ps_{25}	K_{oc}	K_w	S_c	K_{m4}	F_{25}	BP_S	BCF_p	BCF_f
ACE	C22	–	–	−0.68	0.54	–	−0.68	−3.95	−0.67	–	−0.68	–	–	–	–	–	–	–
	C23	–	–	–	0.54	–	–	−3.95	−0.67	–	–	–	–	–	–	–	–	–
	C2f	–	–	−0.68	0.54	–	−0.68	−3.95	−0.67	–	−0.68	–	–	–	–	–	–	1
	C2p	–	–	−0.68	0.54	–	−0.68	−3.95	−0.67	–	−0.68	–	–	–	–	–	1	–
	C43	–	−1	–	0.54	−1.01	–	−3.95	–	–	–	–	–	−1.01	–	–	–	–
PHE	C22	–	–	−0.96	0.87	–	−0.96	−3.75	−0.96	–	−0.96	–	–	–	–	–	–	–
	C23	–	–		0.87	–	–	−3.75	−0.96	–	–	–	–	–	–	–	–	–
	C2f	–	–	−0.96	0.87	–	−0.96	−3.75	−0.96	–	−0.96	–	–	–	–	–	–	1
	C2p	–	–	−0.96	0.87	–	−0.96	−3.75	−0.96	–	−0.96	–	–	–	–	–	1	–
	C43	–	−1		0.87	−1.01		−3.75	–	–	–	–	–	−1.01	–	–	–	–
CHR	C22	0.78	–	−1	–	–	−1	−159.577	−1	−0.78	−1	0.74	0.74	–	0.78	1.51	–	–
	C23	0.78	–	–	–	–	–	−159.57	−1	−0.78	–	0.74	0.74	–	0.78	1.51	–	–
	C2f	0.78	–	−1	–	–	−1	−159.57	−1	−0.78	−1	0.74	0.74	–	0.78	1.51	–	1
	C2p	0.78	–	−1	–	–	−1	−159.57	−1	−0.78	−1	0.74	0.74	–	0.78	1.51	1	–
	C43	0.78	−1.01		–	−1.01	–	−159.57	–	−0.78	–	0.74	0.74	−1.01	0.78	1.51	–	–
BaP	C22	0.93	–	−1.01	0.73	–	−1.01	−267.82	−1.01	−0.94	−1.01	0.89	0.89	–	0.93	1.91	–	–
	C23	0.93	–	–	0.73	–	–	−267.82	−1.01	−0.94	–	0.89	0.89	–	0.93	1.91	–	–
	C2f	0.93	–	−1.01	0.73	–	−1.01	−267.82	−1.01	−0.94	−1.01	0.89	0.89	–	0.93	1.91	–	1
	C2p	0.93	–	−1.01	0.73	–	−1.01	−267.82	−1.01	−0.94	−1.01	0.89	0.89	–	0.93	1.91	1	–
	C43	0.93	−1.01	–	0.73	−1.01	–	−267.82	–	−0.94	–	0.89	0.89	−1.01	0.93	1.91	–	–

"–" means SCi < 0.5.

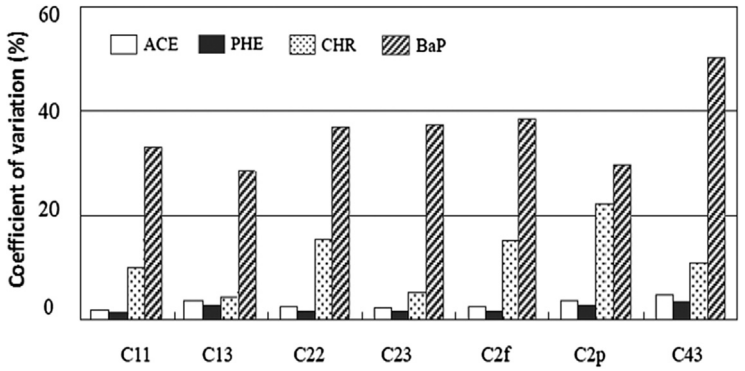

FIGURE 9.8 Comparisons of CV values for the four representative PAHs in the seven subphases.

few FTE models have been applied to solve ecotoxicological problems and perform ecological risk assessments; however, the development is toward a wider application of effect and FTE models (Jørgensen and Fath, 2011).

Through the QWASI fugacity model developed in the present study, the PAHs concentrations in main environmental compartments including the air (air, particulates), water (water, suspended solids, plants, and fishes), and sediment (water and solids) were derived. These results could be used for the ecological risk assessments of PAHs in the Lake Small Baiyangdian. The proposed multimedia fate model could serve as a fundamental for developing an effect model and FTE model to solve ecotoxicological problems and perform ecological risk assessments of PAHs in the Lake Small Baiyangdian. Further, the applications of the effect model and FTE model in the lake would promote the development of ecotoxicological model.

The modeling results in the present study point out that macrophytes play a very important role in maintaining a healthy lake ecosystem by taking up toxic substances and by creating a favorable environment for a variety of complex chemical, biological, and physical processes that contribute to the removal and degradation of toxic pollutants (Xu et al., 1999). Macrophytes growing in a lake are also crucial to regulate lake biological structure, because they limit algal growth by shading and competing for nutrients with algae and because they increase herbivorous fish biomass by providing food and a refuge (Xu et al., 1999).

9.3 CONCLUSIONS

A QWASI fugacity model was developed to characterize the fate and transfer of 15 priority PAHs in Lake Small Baiyangdian. The reliability of the model estimates was evaluated by various means including concentration validation, sensitivity, and uncertainty analysis. There was generally good agreement between the modeled and measured concentrations with the differences within an order of magnitude for the majority of PAH components. The fluxes into and out of the lake as well as each compartment were well balanced. The

average bioaccumulation flux of PAHs by plants was four times higher than that by fishes. The transfer directions of PAHs were from air to water and to sediment. Temperature was the most influential parameter and was more sensitive to the modeled concentrations of middle- and high-molecular-weight PAHs that were considered as the source of the model uncertainty. Overall, the model developed in this study could well characterize the fate and transfer of PAHs in a well-defined ecosystem, i.e., a typical vegetation-dominant lake, which is rarely reported before. This approach provide an illustrative case for fugacity model study within a small scale and open for a wider application of this model approach for future studies.

Acknowledgments

The funding for this study was provided by National Project for Water Pollution Control (2012ZX07103-002), the National Science Foundation of China (NSFC) (41271462, 41030529). This work is also supported by a grant from the 111 Project (B14001).

References

Ao, J.T., Chen, J.W., Tian, F.L., Cai, X.Y., 2009. Application of a level IV fugacity model to simulate the long-term fate of hexachlorocyclohexane isomers in the lower reach of Yellow River basin, China. Chemosphere 74, 370–376.

Arnot, J.A., Gobas, F., 2004. A food web bioaccumulation model for organic chemicals in aquatic ecosystems. Environmental Toxicology and Chemistry 23, 2343–2355.

Baek, J.M., Park, S.J., 2000. Tracking the distribution of organic compounds using fugacity model. Korean Journal of Chemical Engineering 17, 12–16.

Bai, Y.J., 2008. Pollution characteristics of polycyclic aromatic hydrocarbons (PAHs) in surface water in western area around Bohai Bay. Ph.D. Thesis. Peking University, Beijing.

Ballschmiter, K., 1992. Transport and fate of organic-compounds in the global environment. Angewandte Chemie-International Edition in English 31, 487–515.

Banks, R.B., Herrera, F.F., 1997. Effect of Wind and Rain on Surface Reaeration. J. Environ. Engr. Div. ASCE 103 (EE3), 489–504.

Beijing Statistic Bureau, 2005. Beijing Statatistic Year Book. Chinese Statistic Press, Beijing.

Binelli, A., Provini, A., 2003. The PCB pollution of Lake Iseo (N. Italy) and the role of biomagnification in the pelagic food web. Chemosphere 53, 143–151.

Burns, L.A., Cline, D.M., Lassiter, R.R., 1982. Exposure Analysis Modeling System (EXAMS): User Manual and System Documentation. EPA-600/3-82-023. Environmental Research Laboratory, US EPA, Athens, CA.

Calamari, D., Vighi, M., Bacci, E., 1987. The use of terrestrial plant biomass as a parameter in the fugacity model. Chemosphere 16, 2359–2364.

Campfens, J., Mackay, D., 1997. Fugacity-based model of PCB bioaccumulation in complex aquatic food webs. Environmental Science & Technology 31, 577–583.

Cao, H.Y., Liang, T., Tao, S., Zhang, C.S., 2007. Simulating the temporal changes of OCP pollution in Hangzhou, China. Chemosphere 67, 1335–1345.

Cao, H.Y., Tao, S., Xu, F.L., Coveney, R.M., Cao, J., Li, B.G., Liu, W.X., Wang, X.J., Hu, J.Y., Shen, W.R., Qin, B.P., Sun, R., 2004. Multimedia fate model for hexachlorocyclohexane in Tianjin, China. Environmental Science & Technology 38, 2126–2132.

Carsel, R.F., Smith, C.N., Mulkey, L.A., 1984. User's Manual for the Pesticide Root Zone Model (PRZM). release 1, EPA-600/3-84-109. US EPA, Athens, GA.

Chen, J.G., Zhou, W.H., Deng, A.J., Sun, G.H., 2006. Formation and evolution of the longitudinal profile of the Lower Yellow River in modern times. Sediment Study 2 (1), 1–8.

Cohen, Y., 1984. Modeling of Pollutant Transport and Accumulation in a Multimedia Environment. In: The Conference on Geochemical and Hydrologic Processes and their Protection, Council on Environmental Quality, September 25, Washington, DC.

Connolly, J.P., Pedersen, C.J., 1988. A thermodynamic-based evaluation of organic-chemical accumulation in aquatic organisms. Environmental Science & Technology 22, 99–103.

Cowan, C.E., M, D., Feijtel, T.C.J., van de Meent, D., Di Guardo, A., Davies, J., Mackay, N., 1995. The Multi-Media Fate Model: A Vital Tool for Predicting the Fate of Chemicals. SETAC Press, Pensacola, FL.

Davenport, J., 1999. Swimbladder volume and body density in an armoured benthic fish, the streaked gurnard. Journal of Fish Biology 55, 527–534.

Diamond, M.L., MacKay, D., Poulton, D.J., Stride, F.A., 1996. Assessing chemical behavior and developing remedial actions using a mass balance model of chemical fate in the Bay of Quinte. Water Research 30, 405–421.

Diepens, N.J., Arts, G.H.P., Focks, A., Koelmans, A.A., 2014. Uptake, Trans location, and Elimination in Sediment-Rooted Macrophytes: A Model-Supported Analysis of Whole Sediment Test Data. Environmental Science & Technology 48, 12344–12353.

Dong, J.Y., Gao, H., Wang, S.G., Yao, H.J., Ma, M.Q., 2009. Simulation of the transfer and fate of HCHs since the 1950s in Lanzhou, China. Ecotoxicology and Environmental Safety 72, 1950–1956.

Duan, Y.H., 2005. Distribution and source–sink relationship of polycyclic aromatic hydrocarbons in topsoil from Tianjin. Ph.D. Thesis. Peking University, Beijing.

Edwards, F.G., Egemen, E., Brennan, R., Nirmalakhandan, N., 1999. Ranking of toxics release inventory chemicals using a Level III fugacity model and toxicity. Water Science and Technology 39, 83–90.

Gilbertson, M., 1996. Organochlorine contaminants in the Great Lakes. Ecological Applications 6, 966–971.

Gobas, F., Arnot, J.A., 2010. Food web bioaccumulation model for polychlorinated biphenyls in San Francisco bay, California, USA. Environmental Toxicology and Chemistry 29, 1385–1395.

Gobas, F., Wilcockson, J.B., Russell, R.W., Haffner, G.D., 1999. Mechanism of biomagnification in fish under laboratory and field conditions. Environmental Science & Technology 33, 133–141.

Gobas, F., Zhang, X., Wells, R., 1993. Gastrointestinal magnification - the mechanism of biomagnification and food-chain accumulation of organic-chemicals. Environmental Science & Technology 27, 2855–2863.

Hauck, M., Hendriks, H.W.M., Huijbregts, M.A.J., Ragas, A.M.J., van de Meent, D., Hendriks, A.J., 2011. Parameter uncertainty in modeling bioaccumulation factors of fish. Environmental Toxicology and Chemistry 30, 403–412.

HPEPB (Hebei Provincial Environmental Protection Bureau), 2001. Environmental Quality Statement 1996–2000. Hebei Provincial Environmental Protection Bureau, Hebei.

Hu, C.H., Ji, Z.W., Huang, Y.J., Chen, D., 1998. Analysis on dredging practice in rivers, lakes and reservoirs. Journal of Sediment Research 12 (4), 47–55.

Hung, H., Mackay, D., 1997. A novel and simple model of the uptake of organic chemicals by vegetation from air and soil. Chemosphere 35, 959–977.

Jørgensen, S.E., Fath, B.D., 2011. Fundamentals of Ecological Modelling, fourth ed. Elsevier, Amsterdam.

Jørgensen, S.E., Nielsen, S.N., 1994. Models of the structural dynamics in lakes and reservoirs. Ecological Modelling 74, 39–46.

Jin, X.C., 1990. Chemistry of Organic Compound Pollutant. Tsinghua University Press, Beijing.

Karickhoff, S.W., 1981. Semi-empirical estimation of sorption of hydrophobic pollutants on natural sediments and soils. Chemosphere 10, 833–846.

Koelmans, A.A., Van der Heijde, A., Knijff, L.M., Aalderink, R.H., 2001. Integrated modelling of eutrophication and organic contaminant fate & effects in aquatic ecosystems. A review. Water Research 35, 3517–3536.

Kong, X., He, W., Qin, N., He, Q., Yang, B., Ouyang, H., Wang, Q., Yang, C., Jiang, Y., Xu, F., 2014. Modeling the multimedia fate dynamics of γ-hexachlorocyclohexane in a large Chinese lake. Ecological Indicators 41, 65–74.

Kong, X.Z., He, W., Qin, N., He, Q.S., Yang, B., Ouyang, H.L., Wang, Q.M., Yang, C., Jiang, Y.J., Xu, F.L., 2012. Simulation of the Fate and Seasonal Variations of alpha-Hexachlorocyclohexane in Lake Chaohu Using a Dynamic Fugacity Model. Scientific World Journal. http://dx.doi.org/10.1100/2012/691539.

Lang, C., Tao, S., Wang, X.J., Zhang, G., Li, J., Fu, J.M., 2007. Seasonal variation of polycyclic aromatic hydrocarbons (PAHs) in Pearl River Delta region, China. Atmospheric Environment 41, 8370–8379.

Lang, C., Tao, S., Wang, X.J., Zhang, G., Fu, J.M., 2008. Modeling polycyclic aromatic hydrocarbon composition profiles of sources and receptors in the Pearl River Delta, China. Environmental Toxicology and Chemistry 27 (1), 4–9.

Li, Y.L., He, W., Liu, W.X., Kong, X.Z., Yang, B., Yang, C., Xu, F.L., 2015. Influences of binding to dissolved organic matter on hydrophobic organic compounds in a multi-contaminant system: coefficients, mechanisms and ecological risks. Environmental Pollution 206, 461–468.

Liu, Z.Y., Quan, X., Yang, F.L., 2007. Long-term fate of three hexachlorocyclohexanes in the lower reach of Liao River basin: Dynamic mass budgets and pathways. Chemosphere 69, 1159–1165.
Ma, Z.P., Zhao, J.H., Kang, X.J., Jing, A.Q., 2007. The wind-driven water circulation in Baiyangdian Lake, China and the implication to environmental remediation. Oceanologia et Limnologia Sinica 38 (5), 405–410.
Mackay, D., Shiu, W.Y., Ma, K.C., 1997. Illustrated Handbook of Physical–Chemical Properties and Environmental Fate for Organic Chemicals. In: Pesticide Chemicals, Volume V. Lewis Publishers, Boca Raton, FL.
Mackay, D., 1979. Finding fugacity feasible. Environmental Science & Technology 13, 1218–1223.
Mackay, D., 1982. Correlation of bioconcentration factors. Environmental Science & Technology 16, 274–278.
Mackay, D., 2001. Multimedia Environmental Models: The Fugacity Approach, second ed. Lewis Publishers, New York, USA.
Mackay, D., Diamond, M., 1989. Application of the QWASI (quantitative water air sediment interaction) fugacity model to the dynamics of organic and inorganic chemicals in lakes. Chemosphere 18, 1343–1365.
Mackay, D., Fraser, A., 2000. Bioaccumulation of persistent organic chemicals: mechanisms and models. Environmental Pollution 110, 375–391.
Mackay, D., Hughes, A.I., 1984. 3-parameter equation describing the uptake of organic-compounds by fish. Environmental Science & Technology 18, 439–444.
Mackay, D., Joy, M., Paterson, S., 1983a. A quantitative water, air, sediment interaction (QWASI) fugacity model for describing the fate of chemicals in lakes. Chemosphere 12, 981–997.
Mackay, D., Paterson, S., 1981. Calculating fugacity. Environmental Science & Technology 15, 1006–1014.
Mackay, D., Paterson, S., 1982a. Fugacity revisited. Environmental Science & Technology 16, 654A–660A.
Mackay, D., Paterson, S., 1982b. Fugacity revisited - the fugacity approach to environmental transport. Environmental Science & Technology 16, A654–A660.
Mackay, D., Paterson, S., 1991. Evaluating the multimedia fate of organic-chemicals - a Level-III fugacity model. Environmental Science & Technology 25, 427–436.
Mackay, D., Paterson, S., Joy, M., 1983b. A quantitative water, air, sediment interaction (QWASI) fugacity model for describing the fate of chemicals in rivers. Chemosphere 12, 1193–1208.
Mackay, D., Paterson, S., Schroeder, W.H., 1986. Model describing the rates of transfer processes of organic-chemicals between atmosphere and water. Environmental Science & Technology 20, 810–816.
Mackay, D., Paterson, S., Shiu, W.Y., 1992. Generic models for evaluating the regional fate of chemicals. Chemosphere 24, 695–717.
MathWorks, 2002. Using MATLAB Version 6. The MathWorks, Inc, Natick, MA, US.
McKone, T.E., 1996. Alternative modeling approaches for contaminant fate in soils: uncertainty, variability, and reliability. Reliability Engineering & System Safety 54, 165–181.
McKone, T.E., Maddalena, R.L., 2007. Plant uptake of organic pollutants from soil: bioconcentration estimates based on models and experiments. Environmental Toxicology and Chemistry 26, 2494–2504.
Paasivirta, J., Sinkkonen, S., Mikkelson, P., Rantio, T., Wania, F., 1999. Estimation of vapor pressures, solubilities and Henry's law constants of selected persistent organic pollutants as functions of temperature. Chemosphere 39, 811–832.
Paraiba, L.C., Bru, R., Carrasco, J.M., 2002. Level IV fugacity model depending on temperature by a periodic control system. Ecological Modelling 147, 221–232.
Paraiba, L.C., Carrasco, J.M., Bru, R., 1999. Level IV Fugacity Model by a continuous time control system. Chemosphere 38, 1763–1775.
Parajulee, A., Wania, F., 2014. Evaluating officially reported polycyclic aromatic hydrocarbon emissions in the Athabasca oil sands region with a multimedia fate model. Proceedings of the National Academy of Sciences of the United States of America 111, 3344–3349.
Paterson, S., Mackay, D., McFarlane, C., 1994. A model of organic-chemical uptake by plants from soil and the atmosphere. Environmental Science & Technology 28, 2259–2266.
Perry, R.H., Chilton, C.H., 1973. Chemical Engineers' Handbook, 5th edition. McGraw-Hill Book Co., New York, pp. 230–235.
Saloranta, T.M., Armitage, J.M., Haario, H., Naes, K., Cousins, I.T., Barton, D.N., 2008. Modeling the effects and uncertainties of contaminated sediment remediation scenarios in a Norwegian Fjord by Markov chain Monte Carlo simulation. Environmental Science & Technology 42, 200–206.
Schnoor, J.L., Mcavoy, D.C., 1981. Pesticide transport and bioconcentration model. J. of Environ. Engineering – American Society of Civil Engineering 107, 1229–1246.

Sharpe, S., Mackay, D., 2000. A framework for evaluating bioaccumulation in food webs. Environmental Science & Technology 34, 2373–2379.

Shor, L.M., Rockne, K.J., Taghon, G.L., Young, L.Y., Kosson, D.S., 2003. Desorption Kinetics for Field-Aged Polycyclic Aromatic Hydrocarbons from Sediments. Environmental Science & Technology 37 (8), 1535–1544.

STF (Soil Transport and Fate Database and Model Management System), 1991. Environmental Systems and Technologies. Blacksburg, USA.

Tao, S., Cao, H.Y., Liu, W.X., Li, B.G., Cao, J., Xu, F.L., Wang, X.J., Coveney, R.M., Shen, W.R., Qin, B.P., Sun, R., 2003. Fate modeling of phenanthrene with regional variation in Tianjin, China. Environmental Science & Technology 37, 2453–2459.

Tao, S., Cao, J., Wang, W., Zhao, J., Wang, W., Wang, Z., Cao, H., Xing, B., 2009. A Passive Sampler with Improved Performance for Collecting Gaseous and Particulate Phase Polycyclic Aromatic Hydrocarbons in Air. Environmental Science & Technology 43, 4124–4129.

Tao, S., Yang, Y., Cao, H.Y., Liu, W.X., Coveney, R.M., Xu, F.L., Cao, J., Li, B.G., Wang, X.J., Hua, J.Y., Fang, J.Y., 2006. Modeling the dynamic changes in concentrations of γ-hexachlorocyclohexane (γ-HCH) in Tianjin region from 1953 to 2020. Environmental Pollution 139, 183–193.

Tang, M.J., Xu, Z.X., Zuo, Q., Huang, M.H., Tao, S., 2006. Multimedia fate modeling of PAHs in Guangdong Hong Kong, and Macao. Ecology and Environment 15 (4), 670–673.

Ten Hulscher, T.E.M., Vandervelde, L.E., Bruggeman, W.A., 1992. Temperature dependence of Henry's law constants for selected chlorobenzenes, polychlorinated biphenyls and polycyclic aromatic hydrocarbons. Environmental Toxicology and Chemistry 11 (11), 1595–1603.

Tianjin Environmental Protection Bureau (TJEPB), 1991. Environmental Quality Statement. Tianjin Environmental Protection Bureau, Tianjin.

Tianjin Environmental Protection Bureau (TJEPB), 1996. Environmental Quality Statement. Tianjin Environmental Protection Bureau, Tianjin.

Tianjin Environmental Protection Bureau (TJEPB), 2001. Environmental Quality Statement. Tianjin Environmental Protection Bureau, Tianjin.

Thomas, G., Sweetman, A.J., Ockenden, W.A., Mackay, D., Jones, K.C., 1998. Air-pasture transfer of PCBs. Environmental Science & Technology 32, 936–942.

Thibodeaux, L.J., 1996. Environmental chemodynamics: movement of chemicals in air, water, and soil. John Wiley & Sons, INC.

US EPA, 1996. Soil Screening Guidance: Technical Background Document. US Environmental Protection Agency, Office of Emergency and Remedial Response, Washington, 9355.4–17A.

Van Agreren, M.H., Sytze, K., Dick, B.J., 1998. Handbook on Biodegradation and Biological Treatment of Hazardous Organic Compounds. Kluwer Academic Publishers, New York.

Wang, C., Feng, Y., Sun, Q., Zhao, S., Gao, P., Li, B.-L., 2012. A multimedia fate model to evaluate the fate of PAHs in Songhua River, China. Environmental Pollution 164, 81–88.

Wang, R., Cao, H.Y., Li, W., Wang, W., Wang, W.T., Zhang, L.W., Liu, J.M., Ouyang, H., Tao, S., 2011. Spatial and seasonal variations of polycyclic aromatic hydrocarbons in Haihe Plain, China. Environmental Pollution 159, 1413–1418.

Wang, L.S., 1991. Chemistry of Organic Pollutant. Science Press, Beijing.

Wang, L.S., 1993. Chemical Carcinogens. Chinese Environment Science Press, Beijing.

Wang, X.L., Tao, S., Xu, F.L., Dawson, R.W., Cao, J., Li, B.G., Fang, J.Y., 2002. Modeling the fate of benzo a pyrene in the wastewater-irrigated areas of Tianjin with a fugacity model. Journal of Environmental Quality 31, 896–903.

Wania, F., Breivik, K., Persson, N.J., McLachlan, M.S., 2006. CoZMo-POP 2-A fugacity-based dynamic multicompartmental mass balance model of the fate of persistent organic pollutants. Environmental Modelling & Software 21, 868–884.

Wania, F., Mackay, D., 1995. A global distribution model for persistent organic-chemicals. Science of the Total Environment 160-61, 211–232.

Xu, F.L., Jørgensen, S.E., Tao, S., Li, B.G., 1999. Modeling the effects of ecological engineering on ecosystem health of a shallow eutrophic Chinese lake (Lake Chao). Ecological Modelling 117, 239–260.

Xu, F.L., Qin, N., Zhu, Y., He, W., Kong, X.Z., Barbour, M.T., He, Q.S., Wang, Y., Ou-Yang, H.L., Tao, S., 2013. Multimedia fate modeling of polycyclic aromatic hydrocarbons (PAHs) in Lake Small Baiyangdian, Northern China. Ecological Modelling 252, 246–257.

Xu, F.L., Wu, W.J., Wang, J.J., Qin, N., Wang, Y., He, Q.S., He, W., Tao, S., 2011. Residual levels and health risk of polycyclic aromatic hydrocarbons in freshwater fishes from Lake Small Bai-Yang-Dian, Northern China. Ecological Modelling 222, 275–286.

Xu, Z.H., Mao, Z.X., Wang, L.S., Pang, Y.L., 1991. Handbook of Chemistry Property Estimate Method (Environmental Property of Organic Compound). Chemical Industry Press, Beijing.

Yoshida, K., Shigeoka, T., Yamauchi, F., 1987. Multi-phase unsteady state equilibrium model for evaluation of environmental fate of organic chemicals. Toxicological and Environmental Chemistry 15, 159–183.

Yin, J.M., 2008. Chaos characterization of water level and adding solution of water in Lake Bai-Yang-Dian. Masters Thesis. Agricultural University of Hebei.

Zhang, X.L., Tao, S., Liu, W.X., Yang, Y., Zuo, Q., Liu, S.Z., 2005. Source diagnostics of polycyclic aromatic hydrocarbons based on species ratios: A multimedia approach. Environmental Science & Technology 39, 9109–9114.

Zhang, Y., Tao, S., Cao, J., Coveney Jr., R.M., 2007. Emission of polycyclic aromatic hydrocarbons in China by county. Environmental Science & Technology 41, 683–687.

Zhang, Y., Tao, S., Shen, H., Ma, J., 2009. Inhalation exposure to ambient polycyclic aromatic hydrocarbons and lung cancer risk of Chinese population. Proceedings of the National Academy of Sciences of the United States of America 106, 21063–21067.

Zhao, F., 1995. Baiyangdian large aquatic resource survey and the impact of eutrophication. Journal of Environmental Sciences 16, 21–24.

Zhao, X., Cui, B.S., Yang, Z.F., 2005. A study of the lowest ecological water level of Baiyangdian Lake. Acta Ecologica Sinica 25 (5), 1033–1040.

Zhao, Y.H., Lian, J.Y., Zhao, X.P., 2007. Protection for habitat security of biological resources in wetland of Baiyangdian Natural Reserve. Journal of Shijiazhuang Vocational Technology Institute 17 (2), 1–4.